# 7. Migratory properties of plasmacytoid dendritic cells

## 7.1. Introduction

As part of the innate immune defense, one of the major functions of pDCs is to sense invading microbial pathogens. Under homeostatic conditions (steady-state), immature pDCs are distributed in the blood, in lymphoid organs (including the bone marrow, spleen and lymph nodes), and they are found in peripheral tissues such as the liver, gut and lung, where pathogens are likely to enter. In response to pathogen-detection and "danger signal" -induced inflammation, certain trafficking signals enable pDCs to accumulate in the tissue in increased numbers. While this may be beneficial for the elimination of microbes, pDCs have also been found to infiltrate inflamed organs of systemic lupus erythematosus-(SLE) patients, the synovial fluid of patients with rheumatoid arthritis (RA), and the skin of psoriasis patients [135, 149, 205]. At such inflamed sites, pDCs possibly contribute to disease pathogenesis by secretion of type IFNs and other pro-inflammatory cytokines [147]. While the expression of candidate trafficking molecules on pDCs is partially known, the precise molecular mechanism of how pDCs gain access to organs in the steady-state and to inflammatory sites, and how they migrate through interstitial tissues remain poorly defined.

Leukocyte trafficking (homing) from the blood stream into tissues generally occurs in a highly specific and organized manner mediated by consecutive molecular interactions [125]. The initial rolling is mediated by selectins that can result in firm adherence by chemokine-induced changes in integrins. Blood-borne pDCs express high levels of the adhesion molecule L-selectin (CD62L) [39, 40]. In L-selectin-deficient mice, reduced numbers of pDCs have been found in PLN indicating a role for this molecule in trafficking of pDCs to lymphoid organs [40]. However, L-selectin blockade by neutralizing antibodies inhibited only the mobilization of pDCs from the bone marrow into the circulation, but not their migration across HEV [131]. These contradictory results could be explained by the source of pDCs, as the first study used pDCs generated by culturing BM cells in the presence of Flt-3L, while the latter used purified cells from the blood. Diacovo et al. showed that BM-derived

pDCs entered PLN under homeostatic conditions only in small numbers, but efficiently transmigrated into PLN during inflammation [129]. Rolling of pDCs on HEV of inflamed PLN was mediated by L- and E-selectin [129]. pDCs also express $\alpha_4\beta_1$ (VLA-4), $\alpha_5\beta_1$ (VLA-5), and $\beta_2$-integrins (LFA-1), receptors for vascular cell adhesion molecule-1 (VCAM-1), fibronectin, and ICAM-1/2, respectively [129, 130]. It was shown that pDCs from LFA-1-deficient mice transferred into WT mice that were pretreated with anti-VCAM-1 antibody were unable to firmly adhere to inflamed HEVs, while rolling was unaffected [129]. These results indicated that $\beta_1$- and $\beta_2$-integrins mediate firm attachment of pDCs to HEVs in inflamed LNs. Furthermore, pDCs express the chemokine receptors CXCR3, CCR2, CCR5, CXCR4 and the newly identified chemokine-like receptor-1 (CMKLR1/Chem23/DEZ) [116, 121, 131, 135, 136]. Upon maturation, and similar to activated mDCs, pDCs upregulate the expression of CCR7, which facilitates DC entry into lymphatic vessels, and subsequent migration to draining PLN [128]. CCR7 may also direct the migration and localization of activated pDCs within lymphoid tissue [128].

In this part of the study, the dynamics and molecular mechanisms of pDC homing in the steady state and to inflamed organs were elucidated.

## 7.2. Results

### 7.2.1. Expression pattern of adhesion molecules and chemokine receptors by pDCs

While pDCs have been found to circulate in the blood and to enter inflamed peripheral lymph nodes from the bloodstream, it has remained controversial whether or to what extent they migrate to secondary lymphoid and peripheral organs under homeostatic and inflammatory conditions. A limiting factor for migration experiments is the low number of pDCs that can be isolated from mice. Alternative approaches for generating sufficient numbers of pDCs for such assays include *in vitro* generated, BM-derived pDCs or pDCs generated *in vivo* by the use of Flt-3L (see chapter 1). For the experiments described in this study we chose the latter approach, as pDCs generated by Flt-3L *in vivo* most closely resemble cells found under homeostatic conditions (see chapter 1 and below).

As a first step in our understanding of the molecular mechanisms of pDC migration *in vivo*, we determined the expression of candidate adhesion molecules and chemokine receptors implicated in leukocyte trafficking. We used Affymetrix microarray chips to analyze the RNA expression profile of trafficking molecules in pDCs purified from spleens of Flt-3L treated $DPE^{GFP}xRAG\text{-}1^{-/-}$ mice (see chapter 1). We compared the relative expression levels of homing receptors of immature pDCs (baseline of pDCs cultured in medium for 1 h after sort) to pDCs that had been stimulated with PR8 virus or CpG 1826 ODN. We found several members of the selectin and integrin family to be highly expressed in immature pDCs. These included L-selectin, PSGL-1 and the integrins $\alpha_L$, $\beta_2$, and $\beta_7$ (see Table XIII). CD44 and intercellular adhesion molecule (ICAM)-1 were also expressed, as were CEACAM (carcinoembryonic antigen-related CAM)-1 and 2.

| Adhesion molecule | Relative expression med 1h | fold up/down CPG4h-med4h | fold up/down Flu4h-med4h | fold up/down med4h-med1h |
|---|---|---|---|---|
| CD44 | 10349.6 | 2.3 | 1.4 | 1.1 |
| L-Selectin (Sell) | 4320.4 | 1.0 | 1.6 | 1.7 |
| PSGL-1 (Selp) | 6398.2 | 1.25 | 1.1 | 1 |
| Esl (Glg1) | 381.8 | 1.6 | 1.5 | 1.2 |
| Integrin a4 | 270.2 | 11.0 | 6.9 | 3.3 |
| Integrin a6 | 28.5 | 2.1 | 3.0 | 2.1 |
| Integrin al | 1284.0 | 1.1 | 1.4 | 1.1 |
| Integrin am | 55.3 | 1.2 | 1.5 | 2.3 |
| Integrin av | 242.0 | 1.0 | 1.0 | 1.0 |
| Integrin ax | 550.2 | 1.6 | 1.7 | 1.6 |
| Integrin b1 | 444.8 | 2.6 | 2.1 | 1.2 |
| Integrin b2 | 4885.4 | 1.1 | 1.6 | 1.1 |
| Integrin b5 | 106.9 | 2.1 | 1.2 | 1.3 |
| Integrin b7 | 1036.5 | 2.8 | 1.1 | 1.7 |
| Icam1 | 1213.7 | 3.6 | 3.3 | 1.1 |
| Icam2 | 100.3 | 1.6 | 1.0 | 1.0 |
| Alcam | 409.7 | 9.6 | 2.4 | 1.2 |
| Ceacam1 | 1323.8 | 2.5 | 1.7 | 1.1 |
| Ceacam2 | 1340.0 | 2.6 | 1.1 | 1.2 |
| Pecam | 45.2 | 6.8 | 1.9 | 1.25 |
| Edg6 | 1139.5 | 7.3 | 1.6 | 1.3 |
| Slamf9 | 3394.0 | 2.4 | 1.4 | 1.9 |
| Cdh1 | 3212.6 | 2.5 | 2.8 | 1.1 |
| P-Selectin | 26.7 | n.d. | n.d. | n.d. |
| E-Selectin | 5.9 | n.d. | n.d. | n.d. |
| Integrin a5 | 25.4 | n.d. | n.d. | n.d. |
| Integrin a7 | 10.7 | n.d. | n.d. | n.d. |
| Integrin a8 | 9.3 | n.d. | n.d. | n.d. |
| Integrin a9 | 43.5 | n.d. | n.d. | n.d. |
| Integrin ae | 32.3 | n.d. | n.d. | n.d. |
| Integrin b3 | 6.9 | n.d. | n.d. | n.d. |
| Integrin b4 | 3.5 | n.d. | n.d. | n.d. |
| Integrin b6 | 5.6 | n.d. | n.d. | n.d. |

| Chemokine receptor | Relative expression med 1h | fold up/down CPG4h-med4h | fold up/down Flu4h-med4h | fold up/down med4h-med1h |
|---|---|---|---|---|
| Cmklr1 | 585.3 | 5 | 2.6 | 5 |
| Ccr1l1 | 90.2 | 1.1 | 2 | 1.3 |
| Ccrl2 | 24.8 | 9.6 | 16.6 | 1.1 |
| Ccr1 | 154.5 | 1.1 | 1.1 | 3.3 |
| Ccr2 | 557.5 | 5 | 3.3 | 1 |
| Ccr5 | 807.9 | 1.1 | 2.5 | 1.7 |
| Ccr7 | 75.4 | 51.3 | 10.1 | 1.8 |
| Ccr9 | 2383.2 | 1 | 1.1 | 1.1 |
| Cxcr3 | 1099.1 | 10 | 2.5 | 1.2 |
| Cxcr4 | 1573.1 | 1.25 | 1.4 | 3.3 |
| C3ar1 | 4.8 | 11.4 | 1.1 | 1.2 |
| Cx3cr1 | 140.2 | 1.1 | 1.1 | 1.25 |
| Ccr3 | 4.4 | n.d. | n.d. | n.d. |
| Ccr4 | 5.6 | n.d. | n.d. | n.d. |
| Ccr6 | 49 | n.d. | n.d. | n.d. |
| Ccr8 | 4.1 | n.d. | n.d. | n.d. |

*n.d.: not detectable*

**Table XIII. Expression of adhesion molecules and chemokine receptors in immature and *in vitro* activated pDCs.**

Relative mRNA expression levels of adhesion molecules and chemokine receptors in pDCs cultured in medium for 1 h (med 1 h) are displayed in column 2. Changes in RNA levels are represented by fold values for up- (red) or downregulation (blue) after stimulation with CpG 1826, influenza PR8 virus or control conditions (see chapter 1).

In addition, the expression of chemokine receptors CXCR3, CXCR4, CCR5 and Cmklr1 (chemerin receptor) suggests that immature pDCs have the capacity to migrate to peripheral organs, particularly after the induction of inflammation.

Stimulation with CpG 1826 upregulated the expression of integrin $\alpha_4$ and ALCAM (activated leukocyte CAM). We also found upregulation of CCRL2 and the complement receptor C3aR1, which has been shown to mediate chemotaxis in response to anaphylatoxins [138]. PECAM (platelet/endothelial CAM) was 6.8-fold induced in pDCs upon stimulation with CpG, which could indicate a possible enhanced capacity of activated pDCs to transmigrate through the vessel wall [206]. Downregulation of CXCR3 and high induction of CCR7 in CpG-stimulated pDCs suggests that pDCs gain the ability to home into lymphoid organs via afferent lymphatics similar to activated mDCs [25]. Interestingly, edg6, a receptor for sphingosine-1-phosphate (S1P), was downregulated 7-fold in pDCs after stimulation with CpG 1826, but not after PR8 virus. S1P receptors are involved in retaining cells in tissues [207], suggesting that the downregulation after stimulation may increase pDC egress from tissues. Stimulation of pDCs with PR8 virus induced the expression of integrin $\alpha_4$ and CCR7 much less when compared to CpG 1826. Interestingly, whereas the mRNA-level for the chemerin receptor decreased 5-fold after activation with CpG 1826, influenza virus induced its levels 2.6-fold, suggesting a distinct role for this receptor in the migratory behavior of differentially activated pDCs.

Next, we analyzed the protein expression levels of adhesion molecules on the surface of pDCs. Moreover, to exclude that Flt-3L treatment or the lack of lymphocytes in RAG-$1^{-/-}$ animals could have potentially altered the expression of adhesion molecules, we isolated pDCs from the spleens of $DPE^{GFP}$ mice and compared their expression levels to $DPE^{GFP}$xRAG-$1^{-/-}$ treated mice with or without Flt-3L (Figure 25 and Table XIV). BALB/c mice were included in these analyses, because these mice were used in some of the experiments described below. In agreement with the microarray data, the majority of pDCs highly expressed the $\alpha_4$ integrin chain, CD44, and P-selectin ligands (Figure 25). The proportion of pDCs that expressed these molecules was very similar between the different

mouse strains, indicating that the absence of lymphocytes and/or Flt-3L treatment did not influence the phenotypic profile of pDCs *in vivo*. pDCs isolated from spleens of BALB/c mice and DPE$^{GFP}$xRAG-1$^{-/-}$ mice after Flt-3L treatment revealed higher relative expression levels of L-selectin and $\alpha_4$ integrin as compared to DPE$^{GFP}$ and DPE$^{GFP}$xRAG-1$^{-/-}$ mice (Figure 25 and Figure XIV).

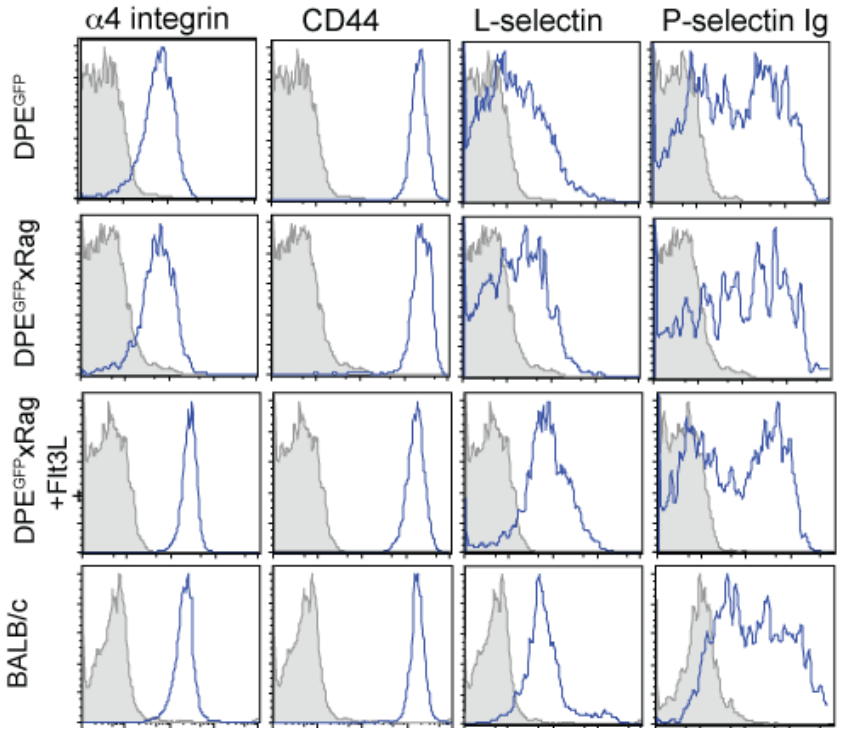


**Figure 25: Expression of adhesion molecules on pDCs.**

Flow cytometric analysis of adhesion molecule expression (blue lines) by pDCs derived from the spleens of the indicated mouse strains (one representative out of 3-5 animals). Grey lines represent isotype control staining. In BALB/c mice, pDCs were defined as CD11c$^{int}$ B220$^{+}$ mPDCA-1$^{+}$ cells. In GFP-transgenic mice, pDCs were identified as GFP$^{hi}$ B220$^{+}$ cells.

In conclusion, immature pDCs express a panel of adhesion molecules and chemokine receptors that facilitates migration to several organs during homeostasis and in inflammation. Differential activation of pDCs *in vitro* with CpG 1826 and PR8 virus induced the transcription of distinct homing molecules primarily for access to PLN via afferent

lymphatics.

### 7.2.2. Differential expression of L-selectin on circulating and splenic immature and activated pDCs

We have shown in chapter 1, that *in vivo* expansion of pDCs with Flt-3L in $DPE^{GFP}xRAG\text{-}1^{-/-}$ mice provided an excellent tool for generating sufficient numbers of pDCs for our studies while maintaining pDCs immature and in their natural environment. In order to study which organs immature pDCs enter from the blood during the steady-state, homing studies require the intravenous injection of cells. As we wanted to transfer splenocytes from $DPE^{GFP}xRAG\text{-}1^{-/-}$ mice harboring $GFP^{+}$ pDCs, we next compared the expression of trafficking molecules on pDCs in the blood-stream as compared to splenic pDCs.

Strikingly, pDCs in the blood exhibited approximately tenfold higher L-selectin expression levels than splenic pDCs (Figure 26A). These results may point towards a differential L-selectin regulation on blood-borne versus tissue-derived pDCs, and may indicate that L-selectin is downregulated upon tissue entry of pDCs. In order to test this hypothesis, splenic pDCs were adoptively transferred by intravenous injection into WT recipients. 24 h later, $GFP^{hi}$ $B220^{+}$ donor cells were isolated from the blood and the spleen of recipient animals. In confirmation of our previous findings, circulating pDCs in peripheral blood expressed ten-fold higher L-selectin levels as compared to cells in the spleen (Figure 26B). It could be possible either that L-$selectin^{hi}$ pDCs selectively migrated into the blood stream or that cells that reach the circulation upregulate L-selectin. In favor of the latter possibility, *in vitro* cultured unstimulated splenic pDCs also upregulated L-selectin surface expression. In contrast, pDCs that had been activated with CpG displayed low levels of L-selectin expression (Figure 26C).

Together, our data indicate that L-selectin is downregulated upon tissue entry of pDCs, while its expression was maintained at high levels on circulating cells in the blood.

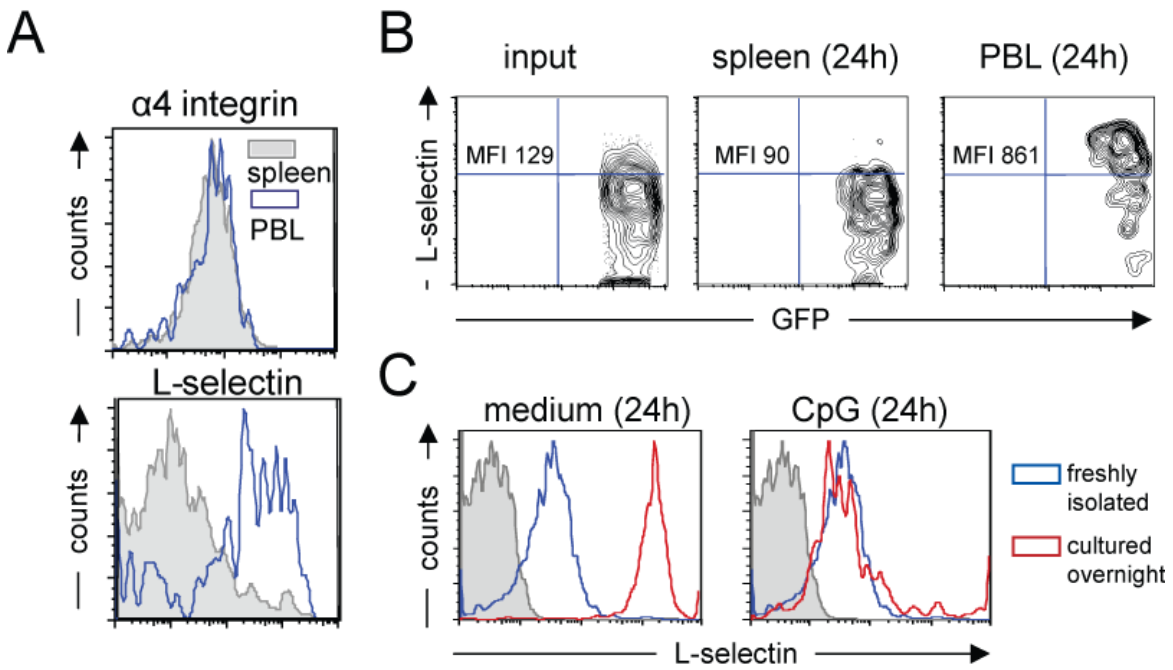


**Figure 26: Circulating pDCs express higher levels of L-selectin compared to splenic pDCs.**

(**A**) Expression of $\alpha_4$-integrin and L-selectin on pDCs freshly isolated from peripheral blood (PBL) and spleen of $DPE^{GFP}$ mice. Gates were set on $GFP^+$ $B220^+$ cells. (**B**) Levels of L-selectin on freshly isolated pDCs as compared to pDCs recovered from spleen and PBL 24 h after adoptive transfer (one out of 3 independent experiments shown). MFI represents the mean fluorescence intensity of the entire pDC population. (**C**) L-selectin expression on pDCs cultured overnight (red histogram) in media alone or in the presence of CPG 1826 (5 µg/ml). Expression on freshly isolated pDCs is shown in comparison (blue histogram). Isotype control is shown in grey.

The expression of adhesion molecules in PBL and spleens of the mouse strains used in this study is depicted below (see Table XIV).

| | | BALB/c | | DPE$^{GFP}$ | | DPE$^{GFP}$x RAG-1$^{-/-}$ | | DPE$^{GFP}$xRAG-1$^{-/-}$ +Flt-3L | |
|---|---|---|---|---|---|---|---|---|---|
| | | % | MFI | % | MFI | % | MFI | % | MFI |
| **L-selectin** | PBL | 91±2 | 990±599 | 78±1 | 552±197 | 70±13 | 364±46 | 82±6 | 418±351 |
| | spleen | 89±4 | 178±44 | 32±0.4 | 54±0 | 31±1 | 52±10 | 71±13 | 144±73 |
| **α4 integrin** | PBL | 100±0 | 212±10 | 94±9 | 118±43 | 91±3 | 83±22 | 100±0.1 | 310±58 |
| | spleen | 100±0.1 | 215±16 | 90±2 | 84±8 | 90±6 | 99±16 | 100±0.1 | 291±1 |
| **CD44** | PBL | 100±0 | 2432±314 | 100±0 | 4158±668 | 100±0 | 4442±905 | 100±0 | 2696±22 |
| | spleen | 100±0.1 | 1843±89 | 100±0 | 3077±141 | 100±0 | 2720±418 | 100±0 | 3262±1930 |
| **P-selectin ligands** | PBL | 50±2 | 536±150 | 58±7 | 339±159 | 58±4 | 439±185 | 60±16 | 963±947 |
| | spleen | 51±1 | 420±168 | 65±11 | 335±7 | 63±0.1 | 437±96 | 50±12 | 469±387 |

**Table XIV. Expression of adhesion molecules on pDCs.**

pDCs in the spleens and PBL from BALB/c, DPE$^{GFP}$, DPE$^{GFP}$xRAG-1$^{-/-}$, or DPE$^{GFP}$xRAG-1$^{-/-}$ treated with Flt-3L mice were analyzed for the expression the indicated adhesion molecules (3-5 mice). In BALB/c mice, pDCs were defined as CD11c$^{int}$ B220$^{+}$ mPDCA-1$^{+}$ cells. In DPE$^{GFP}$ mice, pDCs were identified as GFP$^{hi}$ B220$^{+}$ cells. Shown are the percentage (% ± SEM) of marker positive cells and the mean fluorescence intensity (MFI ± SEM) of marker positive cells.

Collectively, we demonstrated that the majority of pDCs expressed high levels of L-selectin, $\alpha_4$ integrin, CD44, and P-selectin ligands. Differences in the mouse strain background or treatment with Flt-3L appeared to not drastically influence the phenotypic profile of pDCs. Moreover, the percentage and MFI of these molecules was similar in pDCs from blood as compared to splenic pDCs with the exception of L-selectin, which was downregulated in splenic pDCs.

### 7.2.3. Chemotactic response of immature and mature pDCs to CCL21 and CXCL12

We also tested the response of immature pDCs from Flt-3L treated DPE$^{GFP}$xRAG-1$^{-/-}$ mice to chemokines. Splenic pDCs were loaded onto transwell filters, which were placed in medium with and without chemokines, and allowed to migrate for 3 hours. Consistent with previous studies, it could be observed that immature murine pDCs migrated towards the CXCR4 ligand CXCL12 (Figure 27, right graph). After maturation with CpG, pDCs strongly responded to the CCR7 ligand CCL21 (Figure 27, left graph), while maintaining responsiveness to CXCL12. These results corroborate the finding that the mRNA levels of CCR7 are increased in pDCs after activation with CpG (see Table XIII).

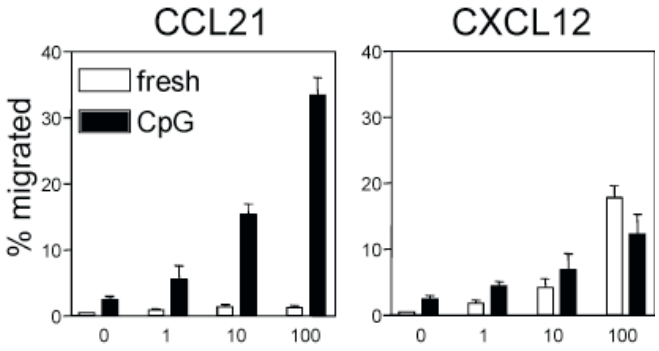


**Figure 27: Chemotactic response of pDCs from Flt-3L treated DPE$^{GFP}$xRAG-1$^{-/-}$ mice.**

Freshly isolated or CpG 1826-treated (5 μg/ml, overnight) spleens from B16-Flt-3L bearing DPE$^{GFP}$xRAG-1$^{-/-}$ mice were loaded on transwell filters and placed into medium containing the indicated concentrations (in nM) of CCL21 and CXC12. Data are expressed as percentage of cells of the input that transmigrated within 3 hours.

### 7.2.4. Homing behavior of immature pDCs

In order to determine the migration pathways of pDCs *in vivo*, homing assays were performed. 5x10$^7$ splenocytes containing 2-4x10$^6$ GFP$^+$ pDCs obtained from B16-Flt-3L treated DPE$^{GFP}$xRAG-1$^{-/-}$ mice were injected intravenously into naïve C57BL/6 recipients. At several time points, organs were harvested and analyzed for the presence of GFP$^{hi}$ B220$^+$ donor cells. After 4 hours, donor pDCs were recovered in greatest numbers from the liver

(data not shown), followed by lungs, spleen and BM (Figure 28B). Over the next 24-96 h, cell numbers decreased in liver and lungs with only a small population remaining at 96 h. While pDC accumulation in the spleen remained constant over the observation period (4 h versus 96 h, p=0.57), their numbers increased by 256% in the BM (p=0.018) and PLN (568%; p<0.001). In order to exclude that Flt-3L treatment changed the migratory properties of pDCs, spleens from untreated DPE$^{GFP}$xRAG-1$^{-/-}$ mice were transferred in a control experiment. It was necessary to pool three spleens (containing 1.8x10$^5$ pDCs), which were then injected into a C57BL/6 recipient mouse. The organ distribution as well as the percentages of pDC recovered from BM, spleen, and PLN were almost identical to those found when pDCs from Flt-3L treated animals were used (data not shown), indicating that Flt-3L treatment does not alter the homing behavior of pDCs.

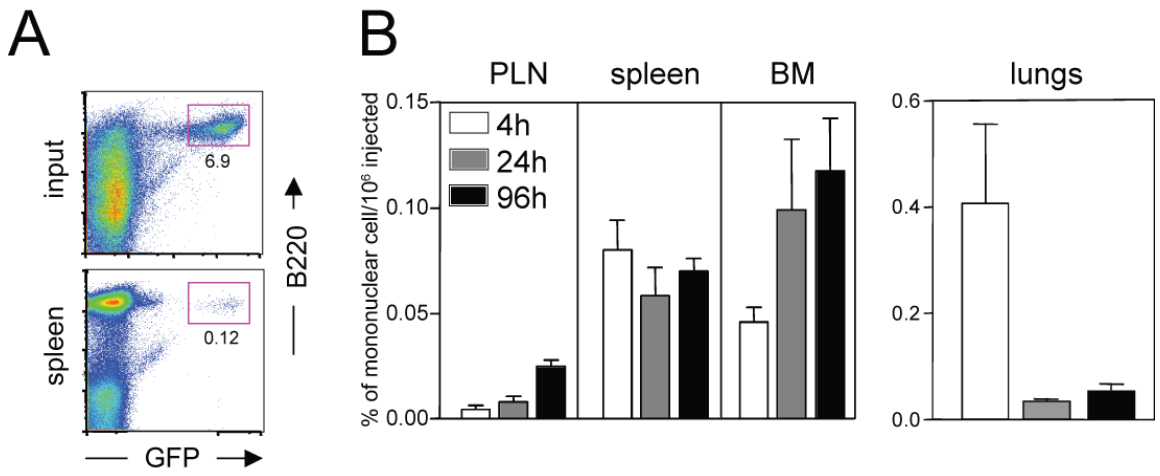


**Figure 28: Homing of blood-borne pDCs under steady state conditions.**

(**A**) Spleens from DPE$^{GFP}$xRAG-1$^{-/-}$ mice injected 12 days earlier with B16-Flt-3L cells served as the input population for homing assays. A total of 4-5x10$^7$ splenocytes containing 2-4x10$^6$ pDCs were injected into the tail veins of naïve C57BL/6 recipient mice. A representative FACS plot of a recipient spleen harvested 24 h later is shown. (**B**) Four, 24, and 96 h after adoptive transfer, the indicated organs were harvested and analyzed for the presence of GFP$^+$ B220$^+$ pDCs (n=3-5 animals per organ and time point). Shown is the percentage (% ± SEM) of pDCs recovered per 10$^6$ injected pDCs (gates were set on live cells).

### 7.2.5. Immature blood-borne pDCs home to the inflamed peritoneal cavity in a $G\alpha_i$-protein coupled receptor-dependent manner

As mentioned above, pDCs have been found in increased numbers at inflammatory sites. However, the kinetics as well as the molecular mechanisms of their migration to inflamed tissues are poorly understood. Using a well-defined model of acute peritonitis [208, 209], we asked whether pDCs accumulated in the peritoneal cavity. Naïve C57BL/6 mice were injected intraperitoneally (i.p.) with incomplete Freund's adjuvant (IFA). Three days later, splenocytes from B16-Flt-3L treated $DPE^{GFP}xRAG\text{-}1^{-/-}$ mice were adoptively transferred into these mice together with purified naïve T cells from $DPE^{DsRED}$ mice as an internal reference population. Cells from the peritoneal cavity and other organs were collected 24 h later. The homing index of $GFP^{hi}$ pDCs and naïve $DsRED^{+}$ T cells was calculated based on the ratio of these populations in the input. A homing index of 1 signifies similar homing of both populations, whereas an index greater than 1 indicates a preferential accumulation of pDCs. Peripheral blood and secondary lymphoid organs harbored considerably more T cells as indicated by the homing index far below 1 (Figure 29B). In contrast, pDCs homed significantly better to the peritoneal cavity, indicating their preferential recruitment to inflammatory sites as compared to naïve T cells (Figure 29A).

Next, we tested whether $G\alpha_i$-protein coupled receptors are involved in pDC migration to the peritoneal cavity. Most of the chemotaxis-mediating receptors are 7-transmembrane proteins that signal via $G\alpha_i$-proteins, which can be selectively blocked by pertussis toxin (PTX). Naïve $DsRED^{+}$ T cells and $GFP^{hi}$ pDCs were treated for 2 hours with PTX prior to adoptive transfer. Consistent with previous findings, PTX treatment abolished homing of naïve T cells to PLN while having no effects on their entry into spleens (Figure 29B; [210]). PTX treatment abrogated the accumulation of pDCs in the inflamed peritoneal cavity with an inverse increase in peripheral blood and spleen, suggesting that their homing to this inflamed tissue was dependent on chemokine receptor signaling (Figure 29B).

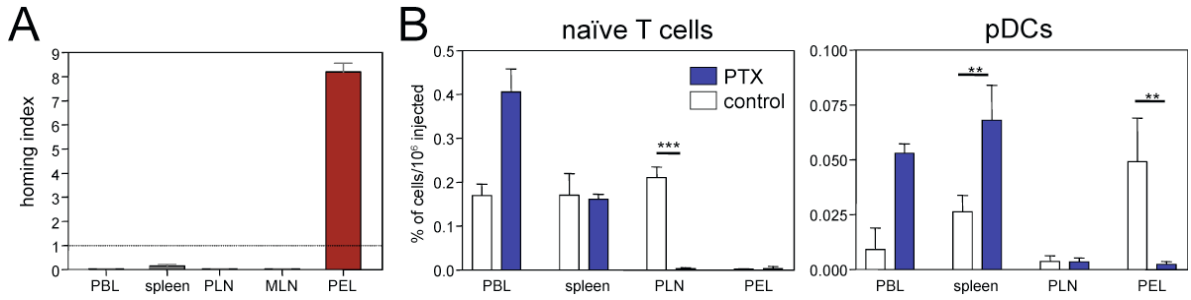


**Figure 29: Homing of pDCs to the inflamed peritoneal cavity is $G\alpha_i$ -dependent.**

(**A**) Peritonitis was induced in naïve C57BL/6 mice by the i.p. injection of emulsified IFA in PBS (0.5 ml; 1:1, vol/vol). Three days later, splenocytes ($5x10^7$) from B16-Flt-3L implanted $DPE^{GFP}xRAG\text{-}1^{-/-}$ mice were mixed with a reference population of $DsRed^+$ naïve T cells ($5x10^6$), and adoptively transferred i.v. into recipient mice. Organs were harvested 24 h later. The homing index was calculated as the ratio of pDCs to naïve T cells recovered from the respective organs corrected for the ratio of both cell types in the input population (n=3 mice). (**B**) $G\alpha_i$-protein coupled receptors were blocked by incubation of naïve T cells and pDCs with pertussis toxin (PTX) (100 ng/ml) for 2 hours prior to adoptive transfer (blue bars). Untreated cells served as controls (open bars). Organs were collected 24 h later. Asterisks indicate statistical significance (unpaired Student's t test).

## 7.2.6. Accumulation of pDCs at sites of inflammation is selectin-dependent

We next asked whether endogenous pDCs accumulate to a similar extent in the inflamed peritoneal cavity, and which adhesion molecules are involved in this process. These experiments were performed in BALB/c mice as pDCs in these mice express similar levels of adhesion receptors as pDCs from Flt-3L treated $DPE^{GFP}xRAG\text{-}1^{-/-}$ mice (Table XIV), thereby making results better comparable to the adoptive transfer studies described above. In addition, the total number of pDCs is larger in the BALB/c background as compared to C57Bl/6 mice. Peritonitis was induced in mice by the injection of Thioglycollate.

As shown in Figure 30A, pDCs accumulated in the peritoneal cavity in a time-dependent manner, whereas pDC numbers remained constant in spleen and blood. Similar kinetics were observed in control experiments performed in $DPE^{GFP}$ mice, with pDCs numbers approximately five-fold lower than in BALB/c animals (data not shown). In order to determine whether the accumulation of pDCs at inflammatory sites was paralleled by their maturation, the phenotype of pDCs isolated from the peritoneal exudate after 24 and 48 h was analyzed. As indicated by low expression levels of CD40, CD80, CD86 and MHC class II molecules, pDCs remained immature in contrast to $CD11c^{hi}$ mDCs, which showed increased level of CD40 and CD86 on their surface (Figure 30B). This finding suggests that the migration of pDCs to inflamed tissues *per se* is not sufficient to drive their maturation, but rather that the presence of specific stimuli, such as TLR ligands, may be necessary for this process.

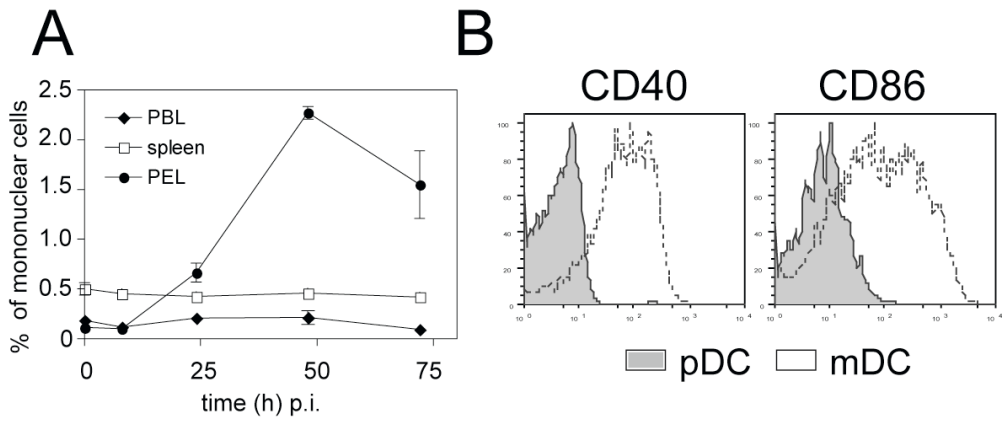


**Figure 30: Immature pDCs accumulate in the inflamed peritoneal cavity.**

(**A**) Peritonitis was induced in BALB/c mice by the injection of Thioglycollate. Peritoneal exudate leukocytes (PEL), spleens, and PBL were harvested at the indicated time points, and analyzed for the presence of pDCs ($CD11c^{int}$ $B220^{+}$ mPDCA-$1^{+}$ Ly6C/$G^{+}$ cells). Symbols represent means ± SEM of 3-5 mice per time point. (**B**) The maturation state of pDCs compared to $CD11c^{hi}$ mDCs isolated from PEL after 24 h was determined by flow cytometry.

When determining the expression of adhesion molecules on pDCs isolated from PEL 24 h after induction of inflammation, we observed that they expressed high levels of $\alpha_4$ integrin and L-selectin, and low levels of $\alpha_4\beta_7$ integrin (Figure 31A). A subset of the cells also expressed ligands for P-selectin, while E-selectin ligand expression was low. Thus, L-selectin represented a valid candidate to mediate migration of pDCs not only into inflamed LNs but also into inflamed peripheral sites. MDCs displayed an opposite expression pattern of these molecules, i.e. low levels of L-selectin and high expression of P- and E-selectin ligands. In order to decipher the role of these molecules in the migration of pDCs into the inflamed peritoneal cavity, we injected blocking antibodies against L-Selectin, P- and E-selectin (Figure 31B). Compared to mice with Thioglycollate-induced peritonitis that received no blocking antibody, we found a 30% increase of pDC numbers after injection of P- and E-Selectin antibodies ($p<0.05$ each). In contrast, anti-L-selectin reduced the number of pDCs in PEL by 34% ($p=0.007$). A combination of anti-L-, P-, and E-selectin further reduced the accumulation of pDCs by 69% as compared to the Thioglycollate-control group ($p=0.001$).

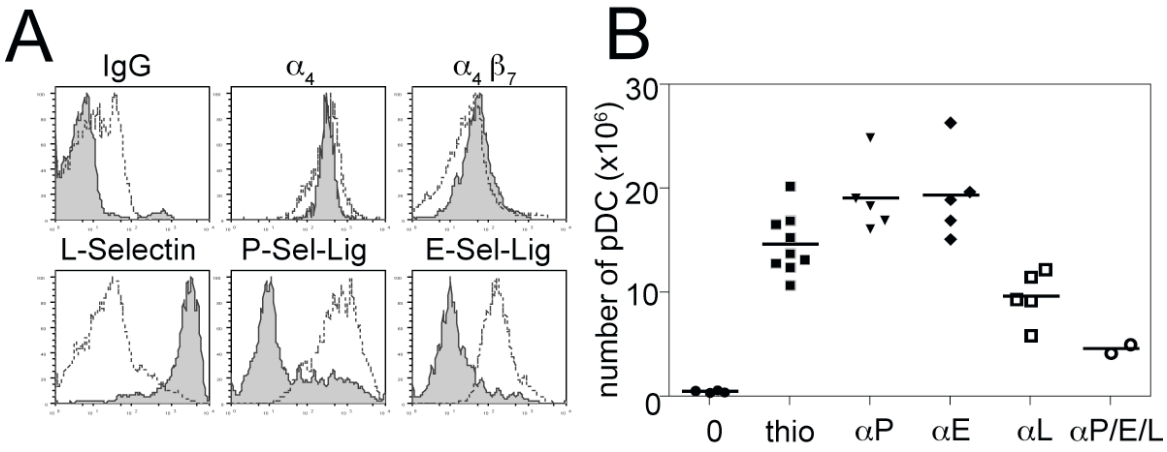


**Figure 31: Selectins are involved in the homing of endogenous pDCs to the inflamed peritoneal cavity.**

Peritonitis was induced in BALB/c mice by the injection of Thioglycollate. (**A**) shows representative FACS profiles (out of 5 mice) of adhesion molecule expression on pDCs identified as $CD11c^{int}$ $B220^{+}$ mPDCA-$1^{+}$ Ly6C/$G^{+}$ cells (grey) and $CD11c^{hi}$ mDCs (open) isolated from the peritoneal cavity after 24 hours. (**B**) Mice were injected with blocking antibodies against selectins alone or in combination (100 $\mu$g at the time of Thioglycollate injection, and 50 $\mu$g 12 h later). PEL were harvested 24 h later and the numbers of pDCs assessed. Zero: naïve mice. Symbols represent individual mice. Bar represents mean.

## 7.3. Discussion

This part of the study was performed to investigate the migratory behavior of pDCs in the steady-state and under inflammatory conditions. In order to better understand the molecular cues mediating trafficking of pDCs, we used microarrays to analyze the global mRNA expression pattern of adhesion molecules and chemokine receptors of immature pDCs. The results revealed the expression of a broad panel of adhesion molecules and chemokine receptors that are transcribed in immature pDCs (Table XIII). We also showed cell surface expression of L-selectin, CD44 and $\alpha_4$ integrins at high levels (Figure 25 and Table XIV). The results from this profiling approach suggest that pDCs express homing receptors that support trafficking into lymphoid organs as well as peripheral (inflamed) tissue. These results may provide an explanation for and an extension of previous observations that pDCs are distributed in small numbers in almost all organs including secondary lymphoid organs and bone marrow, liver, lungs, and intestinal mucosa (Figure 11 in chapter 1 and data not shown) [40-42].

In homing assays, spleens of Flt-3L-treated $DPE^{GFP}xRAG\text{-}1^{-/-}$ mice containing $GFP^{hi}$ pDCs were adoptively transferred and were subsequently tracked in recipient mice by identification of GFP expression (Figure 28A). This system has major advantages as it prevents potential alteration of cell functions by labeling procedures with fluorescent/radioactive dyes. Four hours after adoptive transfer, large numbers of pDCs could be recovered from lungs and livers (Figure 28B and data not shown), indicating that pDCs are capable of entering peripheral organs from the blood stream. This early accumulation in liver and lungs may be due to passive trapping of the cells after intravenous injection, which is commonly observed in homing assays [209]. Over the following 20 hours, pDC numbers decreased in these organs (Figure 28B). Nevertheless, between 24 and 96 h a stable pDC population consolidated in lungs and liver. These data support the hypothesis that pDCs are

recruited from the blood into tissues rather than from differentiation or proliferation *in situ* of organ-resident cells.

The homing assays provide evidence that adoptively transferred pDCs entered PLN at low numbers (Figure 28B), and localized to the T cell areas in the spleen (data not shown). Interestingly, the numbers of pDCs accumulating in PLN increased over a 96 h observation period. This phenomenon could explain why a previous study reported that pDCs are unable to home to non-inflamed lymph nodes after 6 h and 12 h, time points that may have been insufficient for the cells to enter the tissue [129]. Similarly, Yoneyama et al. harvested PLN only 2 h after adoptive transfer of fluorescently labeled pDCs [131]. Also, the study by Diacovo et al. used *in vitro*-cultured BM-derived pDCs that may differ from their *in vivo* counterparts in terms of their trafficking properties. The time-dependent accumulation of pDCs in PLN and BM may reflect changes of their homing molecules over time. We observed that pDCs harvested from spleens of Flt-3L induced mice expressed intermediate levels of L-selectin as compared to higher levels of L-selectin on pDCs isolated from the blood or after resting culture over night (Figure 26A-C). Since L-selectin is required for homing to lymphoid organs, it is likely that higher levels of this molecule positively impact the observed entry of pDCs into PLN. Further studies will be needed to decipher what factors regulate the level of L-selectin and possibly other homing molecules in tissue-resident versus circulating pDCs in the blood.

As mentioned above, circulating pDCs are not only equipped with the PLN homing receptor L-selectin, but also express high levels of molecules implicated in leukocyte trafficking to inflammatory sites (i.e. CD44, $\alpha_4$ integrin, P-selectin ligand(s), and LFA-1). In addition, they express a large panel of chemokine receptors that potentially bind chemoattractants present at sites of inflammation (Table XIII, Table XIV, Figure 25 and data not shown), including CCR5, the chemerin receptor (Cmklr1), CXCR4 and CXCR3, whose ligands (CXCL9/MIG, CXCL10/IP-10, and CXCL11/I-TAC) are induced during viral infections/sites of inflammation [132, 134, 211]. Others have shown that pDCs migrate *in*

*vitro* in response to CXCR4 ligand SDF-1α and CCR5 ligands [129, 131]. CXCR3 ligands promoted pDC migration into draining lymph nodes in a model of cutaneous HSV-infection [131] and induced a chemotaxis response when simultaneously engaged with CXCR4 [134]. Consistent with previous reports, we observed that immature pDCs responded to the CXCR4 ligand CXCL12, while migration towards the CCR7 ligand CCL21 required maturation of the cells (Figure 27). We demonstrated that CpG-activated pDCs upregulate CCR7 (similar to mature myeloid DC), which may facilitate increased influx of pDCs into lymphatic vessels and trafficking to draining lymph nodes (Table XIII). In order to determine whether pDCs are part of the cellular composition of the lymph, one could conduct experiments to collect lymph fluids by cannulation of the thoracic duct. If pDCs were found in the lymph, it would suggest that they recirculate similar to T cells. This would be interesting in light of the surveillance paradigm indicating that pDCs enter and exit organs in constant search of antigens.

While others have identified the mechanisms that mediate pDC recruitment into inflamed lymph nodes [129, 131], the results presented in this part of the study analyzed important steps of pDC homing to sites of inflammation. As compared to naïve T cells, which preferentially circulate through lymphoid organs and are mostly absent in peripheral tissues [209], competitive homing assays revealed a marked predilection of pDCs to migrate to the inflamed peritoneal cavity (Figure 29A and B). PDCs isolated from the site of inflammation expressed a panel of adhesion molecules very distinct from myeloid DCs, as they expressed high levels of L-selectin and only a small subset was P- and E-selectin ligand$^+$ (Figure 31). We demonstrated that pDC homing to the peritoneal cavity was mostly dependent on L-selectin. A combination of three selectin-blocking antibodies could further decrease this effect (Figure 31). These results are largely consistent with the involvement of L- and E-selectin in the homing of BM-derived pDCs to inflamed PLN. Moreover, treatment of pDCs with pertussis toxin prior to the homing assay could inhibit migration to the peritoneal cavity, indicating that $G\alpha_i$-coupled receptor(s) are involved in the process of homing to sites of inflammation (Figure 29B). Future studies will be performed to address

the contribution of specific chemokine receptors. Based on the observation that pDCs (in contrast to mDCs) did not upregulate activation markers in the absence of pathogens at inflammatory sites (Figure 30B) it could be hypothesized that mere extravasation is insufficient to induce the maturation of these cells. Rather, this would require the presence of specific TLR ligands that rapidly result in the induction of costimulatory molecules as well as production of pro-inflammatory mediators (see chapter 1). Since pDCs may be a normal part of the inflammatory infiltrate at any given site of inflammation, this may represent a tissue protective mechanism in the absence of viruses or bacteria.

In summary, we have analyzed the migratory properties of immature pDCs, which express a variety of adhesion molecules and chemokine receptors that allow for their migration into lymphoid and non-lymphoid organs alike. L-selectin appears to be a major homing molecule mediating their accumulation at sites of inflammation.